

GPS Navigation in a High Drag Environment: Applications to Global Precipitation Measurement and Drag-Free Control Concepts

Bo J. Naasz

June 27, 2003

PIP Level II Final Report

Goddard Space Flight Center

Flight Dynamics Analysis Branch, code 595

Introduction

Global Precipitation Measurement (GPM) is a NASA Earth Observing System (EOS) Program mission, currently in the formulation phase. The mission seeks to improve climate prediction, as well as weather and precipitation forecasts by providing highly accurate, near-global measurement of precipitation.

The GPM mission (specifically, the onboard radiometer) requires the spacecraft to maintain its orbital semi-major axis to within 1 km, since less calibration of science data is required if most of the data is taken at relatively similar altitudes. This orbit maintenance will be accomplished on GPM using onboard navigation using the Global Positioning System (GPS) and the New Millennium Program's (NMP) Autonomous Onboard Formation Flying Software (AutoCON) to perform an orbit raising maneuver once every few days. The frequency of these maneuvers will vary throughout the mission as a function of solar flux, ranging from about one maneuver per week to one maneuver per day.

AutoCON was first used on the EO-1 mission to autonomously maintain the spacecraft's orbit relative to Landsat-7 (LS-7).³ EO-1 currently flies in a circulation orbit about a reference trajectory defined relative to the Landsat-7 orbit. Because EO-1 has a slightly lower ballistic coefficient than LS-7, atmospheric drag forces the EO-1 orbit to decay more rapidly than the LS-7 orbit. The EO-1 circulation orbit is a relative trajectory which is initialized with EO-1 positioned ahead of, and above the reference trajectory. As the EO-1 orbit decays, the spacecraft follows a curved path around the reference orbit, called a circulation orbit. The AutoCON software can autonomously perform the orbital maneuvers required to reestablish the EO-1 circulation orbit whenever EO-1 moves outside of the established control box or Landsat-7 performs a maneuver.

The heritage of the AutoCON software, and the parallels between the EO-1 formation flying circulation orbit and the GPM autonomous drag compensation concept make a slightly modified version of AutoCON an excellent fit for GPM. Just as EO-1 autonomously maneuvers to remain within a control box defined relative to LandSat-7, GPM can autonomously maneuver to remain within a semi-major axis–eccentricity control box defined by the science mission requirements.

The primary goal of this work is to demonstrate the use of GPS-based onboard navigation and control to meet the orbital maintenance requirements of GPM. This task is separated into

two major categories: 1) implementation of onboard navigation using the GPS Enhanced Onboard Navigation System (GEONS);² 2) development and implementation of a one-apogee-burn control strategy for GPM.

The secondary goal of this work is to determine the effect of drag-free control on GPS-based navigation accuracy. This goal is related to the primary goal in that it allows us to explore the effects of drag, and other navigation error sources, on the navigation system. The insight gained from this work serves directly to improve our understanding of GPS-based navigation for any spacecraft in an elevated drag regime.

In the following sections we discuss onboard navigation issues, and related GEONS implementation issues. We then describe the simulation approach, including generation of high fidelity truth trajectories, generation of realistic GPS pseudorange measurements, and the processing of those measurements in GEONS. Next, we present the results of the Drag Free Control Analysis. We then discuss the GPM guidance and control strategy, and present navigation simulation results.

Onboard Navigation

The GPS Enhanced Onboard Navigation System (GEONS) uses an Extended Kalman Filter (EKF) to combine real-time measurements from sources such as ground stations, GPS receivers, inter-satellite ranging devices, and celestial navigation sensors with the dynamical equations of motion to precisely estimate the user spacecraft orbital state.

There are a number of sources of error in onboard navigation that are relevant to the GPM guidance, navigation and control strategy. The following error sources are of particular interest: gravity model error, receiver clock error, linearization, atmospheric density and drag model error, ionospheric delay, and actuator error. A significant part of this work was devoted to isolating these error sources in order to gain a more thorough understanding of their effect on navigation accuracy. The end result is a new set of GEONS filter parameters which serve as an excellent starting point for filter optimization for a variety of orbital conditions.

Simulation

Simulation of data for this analysis can be broken into two steps: 1) generation of precise truth trajectories; 2) generation of realistic measurement data.

Truth trajectories for this study are generated using FreeFlyer, a high fidelity spacecraft simulation environment. Force modeling in FreeFlyer includes a 70x70 Earth gravity model, sun and moon gravitation, and a Harris-Priester drag model with a 10.7-centimeter solar flux value of 200. The simulations assume a 3000-kg spacecraft, with drag area of 15 square meters. FreeFlyer is used to generate ephemeris files for the required trajectories.

Measurement data are generated based on the FreeFlyer trajectories using the Measurement Data Simulation Program (DataSim).⁵ GPS pseudoranges with measurement noise standard deviation of 2 meters and clock errors from a Rubidium clock and a temperature compensated crystal oscillator (TCXO) clock are created and stored in the Receiver Independent Exchange (RINEX) format.⁴

For each trajectory and clock combination, 10 random sets of trajectory initial conditions, clock noise, and pseudorange measurement noise are generated. While this does not provide a large Monte Carlo confidence interval, it does allow us to verify proper filter response to a variety of inputs.

Drag Free Trajectory Analysis

Recent work at Goddard Space Flight Center⁶ has demonstrated that spacecraft drag-free control can significantly reduce fuel consumption, and improve the long term predictability of spacecraft orbits. Using a drag-free sensor, a spacecraft can continuously remove the effect of atmospheric drag. Because atmospheric density (and thus drag) are difficult to predict accurately, it is possible that drag-free control could provide improved navigation accuracy. To determine the effect of drag-free control on navigation accuracy, we use GEONS to process simulated GPS pseudorange data for circular orbits with altitudes of 250 km and 450 km, both with and without drag. The orbits without drag approximate spacecraft performing continuous drag-free control about some proof mass. The orbits with drag represent a spacecraft that is either uncontrolled, or performing infrequent, periodic drag-makeup maneuvers.

Table 1 summarizes the GEONS navigation simulations performed in this study. Each simula-

tion is described by a RunID with the following format: $DF-abcde$, where; the value of a describes the altitude of the circular orbit, with 1 = 250km, and 2 = 450km; the value of b describes the drag model, with 1 = drag-free, and 2 = modified Harris-Priester drag;^{2,7} the value of c describes the clock model used, with 1 = no clock error (not included), 2 = Rubidium clock, and 3 = TCXO clock; the value of d describes the ionosphere model, with 1 = no ionospheric delay, and 2 = ionospheric delay modelled in DataSim (we have omitted ionospheric delay for this study, as the bulk of the error introduced by ionospheric delay can be removed by including an appropriate model in the filter); the value of e varies to describe 10 random samples of the initial condition error, clock seed, and pseudorange measurement noise seed.

Table 1: Summary of drag-free control Analysis simulations

RunID	Altitude		Drag Model		Clock Model	
	250km	450km	None	Harris-Priester	Rubidium	TCXO
$DF-1121^*$	×		×		×	
$DF-1131^*$	×		×			×
$DF-1221^*$	×			×	×	
$DF-1231^*$	×			×		×
$DF-2121^*$		×	×		×	
$DF-2131^*$		×	×			×
$DF-2221^*$		×		×	×	
$DF-2231^*$		×		×		×

Tables 2 and 3 show the navigation accuracy results for 80 GEONS simulations. The “mean of mean” values are calculated by averaging the mean error across the 10 sample ensemble at each instance in time. The “mean of standard deviation” values are calculated by averaging the standard deviation of the 10 sample ensemble at each instance in time.

The position and velocity error results presented in Table 2 differ by less than 1% between cases with drag and without drag. For example, comparing the mean position error for the 250-km altitude cases with Rubidium clock noise (RunID numbers $DF-1121$ and $DF-1221$), we see a position accuracy improvement of about 0.47%. This result suggests that continuous drag-free control would not dramatically affect the navigation accuracy for a spacecraft using GPS-based onboard navigation. Another possible explanation of this lack of navigation accuracy improvement is insufficient fidelity in the true drag model. Atmospheric drag is difficult to model accurately, as we have poor knowledge of the true atmospheric density, and spacecraft ballistic coefficient.

Table 2: Ensemble mean-of-mean and mean-of-standard deviation (STD) values for position, velocity and drag coefficient estimation error (parentetic values are base 10 exponents)

RunID	Position Error [m]		Velocity Error [cm/s]		Drag Coefficient Error	
	mean	STD	mean	STD	mean	STD
<i>DF-1121*</i>	3.192(-1)	1.608(-1)	1.965(-1)	8.801(-2)	1.656(-4)	1.150(-3)
<i>DF-1131*</i>	3.016(-1)	1.535(-1)	1.853(-1)	7.816(-2)	1.953(-4)	1.109(-3)
<i>DF-1221*</i>	3.207(-1)	1.625(-1)	1.976(-1)	8.890(-2)	5.555(-2)	2.954(-3)
<i>DF-1231*</i>	3.028(-1)	1.561(-1)	1.862(-1)	7.965(-2)	5.553(-2)	2.925(-3)
<i>DF-2121*</i>	2.399(-1)	1.139(-1)	9.557(-2)	3.817(-2)	1.144(-2)	1.147(-2)
<i>DF-2131*</i>	2.374(-1)	1.154(-1)	9.545(-2)	3.728(-2)	1.149(-2)	1.118(-2)
<i>DF-2221*</i>	2.397(-1)	1.139(-1)	9.554(-2)	3.821(-2)	5.833(-2)	1.321(-2)
<i>DF-2231*</i>	2.373(-1)	1.152(-1)	9.542(-2)	3.728(-2)	5.826(-2)	1.293(-2)

Table 3: Ensemble mean-of-mean and mean-of-standard deviation (STD) values for clock bias and clock drift estimation error (parentetic values are base 10 exponents)

RunID	Clock Bias [m]		Clock Drift [cm/s]	
	mean	STD	mean	STD
<i>DF-1121*</i>	2.120(-2)	2.924(-1)	7.756(-5)	9.775(-4)
<i>DF-1131*</i>	3.035(-1)	8.343(-1)	2.048(-3)	5.814(-1)
<i>DF-1221*</i>	2.180(-2)	2.933(-1)	7.741(-5)	9.778(-4)
<i>DF-1231*</i>	3.048(-1)	8.366(-1)	2.603(-3)	5.812(-1)
<i>DF-2121*</i>	4.672(-3)	2.714(-1)	8.274(-5)	9.765(-4)
<i>DF-2131*</i>	2.876(-1)	7.928(-1)	4.366(-3)	5.667(-1)
<i>DF-2221*</i>	4.923(-3)	2.713(-1)	8.276(-5)	9.764(-4)
<i>DF-2231*</i>	2.871(-1)	7.927(-1)	4.323(-3)	5.666(-1)

To model the uncertainty in these parameters correctly, we must generate a truth trajectory for which the drag does not agree directly with the modelled drag in the filter. In this study, the truth trajectory is based on a modified Harris-Priester drag model, which uses a table look-up to find the atmospheric density at the spacecraft’s position. The filter drag model is also a modified Harris-Priester model, but with an analytical atmospheric density approximation. The truth and filter density models have been shown to disagree by up to 15%.⁷ This drag model difference could be too small, and thus might not completely capture the effect of poorly modelled drag. Future iterations of this work will include more varied truth and filter drag models, either by using a different true drag model or by forcing variation in the truth model’s solar flux value (a parameter that greatly affects the atmospheric density).

Global Precipitation Measurement Analysis

To simulate GPM onboard guidance, navigation, and control (GNC), we use the same simulation procedures described above, with added guidance and control logic to maintain the spacecraft orbit. In this section, we define the GPM guidance law, a simple one-apogee-burn control law, and analyze the effect of this guidance and control strategy on GPS-based navigation using GEONS.

Guidance

The guidance law (the logic by which the spacecraft determines its desired orbit) in this study is a simple mean semi-major axis – mean eccentricity control box. This means that control law must regulate the mean semi-major axis (SMA) and the mean eccentricity to keep them within some predetermined bounds. The control box maximum SMA is 6778km. The minimum SMA varies in four sample trajectories such that the mean orbital altitude is allowed to decay due to drag forces by 1km, 500m, 100m, and 10m before a maneuver is performed. The control box mean eccentricity bounds are fixed at $[0, 0.0001]$.

Control

To define a control law for GPM, we first define the equations of motion for the mean SMA and mean eccentricity. Including only the effects of orbit-control thrust acceleration in the velocity direction, u_v , and atmospheric drag, a_d , the equations of motion are as follows:¹

$$\begin{bmatrix} \dot{a} \\ \dot{e} \end{bmatrix} = \begin{bmatrix} \frac{2a^2v}{\mu} \\ \frac{2(e+\cos\nu)}{v} \end{bmatrix} (u_v + a_d) \quad (1)$$

where a , v , μ , e , and ν are the mean SMA, the orbital speed, the gravitational parameter, the mean eccentricity, and the true anomaly, respectively. The acceleration due to atmospheric drag is

$$a_d = -\frac{1}{2}C_D \frac{A}{m} \rho v_a^2 \quad (2)$$

where C_D , A , m , ρ , and v_a are the drag coefficient, drag area, spacecraft mass, atmospheric density, and orbital speed relative to the atmosphere, respectively.

If the atmospheric drag were exactly known, and the spacecraft actuators were perfectly throttleable, the open loop drag-free control would be simply $u_v = -a_d$. Realistically, the atmospheric drag is known quite poorly due to uncertainties in all of the variables in Eq. (2).⁸ Furthermore, the orbit control thrusters employed by most spacecraft are neither throttleable nor capable of providing the minute levels of thrust required to counter the drag force exactly. The variability of atmospheric conditions, coupled with a small enough semi-major axis control box, makes a strict periodic control schedule unappealing, as it is virtually impossible to predict when orbit reboost maneuvers will be required (this is mostly due to unpredictable solar weather). For these reasons, it is beneficial to develop an autonomous closed loop control based on state errors determined via onboard navigation.

From Eq. (1), velocity direction thrust acceleration at apogee (where $\nu = \pi$) results in increasing mean SMA and decreasing mean eccentricity. Replacing \dot{a} with Δa , and u_v with ΔV in Eq. (1), the apogee ΔV required to raise the mean SMA by Δa kilometers is

$$\Delta V_1 = \Delta a \frac{n(1-e)}{2\eta} \quad (3)$$

where $\eta = \sqrt{1-e^2}$. Similarly, the maximum ΔV for which the final eccentricity will be less than 0.0001 is

$$\Delta V_2 = -\Delta e \frac{na}{2\eta} \quad (4)$$

where

$$\Delta e = -0.0001 - e \quad (5)$$

Eq. (5) assumes that the apogee burn raises the initial perigee to a level higher than the initial apogee (thus making the initial apogee point the final perigee point), such that the final mean eccentricity is 0.0001.

To perform the one-apogee-burn control strategy, we allow the mean SMA to decay by Δa and then apply the lesser of ΔV_1 and ΔV_2 . The result is a maneuver which raises the mean semi-major axis either all the way to 6778 km, or as high as possible such that the resulting mean eccentricity

does not exceed 0.0001. Note that $\Delta V_1 \leq \Delta V_2$ requires that

$$\frac{\Delta a}{a} \leq -\frac{\Delta e}{1-e} \quad (6)$$

This constraint limits the maximum value of Δa or the maximum target eccentricity (which cannot be too small), or both, in a way that favors more frequent maneuvers for spacecraft requiring smaller eccentricities. This observation would force GPM to perform maneuvers more frequently than the rate defined by $\Delta a = 1\text{km}$ if a more circular orbit is required.

Figure 1 illustrates the mean semi-major axis and mean eccentricity response to the one-apogee-burn control strategy, with $\Delta a = 1\text{ km}$. In the 10-day simulation, the control requires four apogee maneuvers (at hours 51, 111, 164, and 226) to maintain the target semi-major axis. All of these maneuvers achieve the target SMA of 6778 km except the one at 111 hours which falls 80 m short of the target. For this maneuver, $\Delta V_2 < \Delta V_1$, and the control applies the lesser of the two, so that the mean eccentricity after the burn is not greater than 0.0001. Note that once the ΔV is completed, the mean eccentricity drifts to a value of almost 0.0002 before the next maneuver is commanded. This result is not surprising, as the control logic regulates only the eccentricity immediately following a maneuver.

The optimal two-burn maneuver (Hohmann transfer) for a 1-km orbit raising maneuver of this kind requires a ΔV of approximately 0.566 m/s. The corresponding one-apogee-burn maneuver for GPM requires an average ΔV of approximately 0.574 m/s.

Figure 2 illustrates the same mean semi-major axis, mean eccentricity information, but with a maximum Δa of only 100 m. This plot shows how increasing maneuver frequency results in an overall decrease in the mean eccentricity. The plot also shows the natural variability of the mean orbital elements. Immediately following each of the maneuvers in this simulation, the mean semi-major axis is within meters of 6778 km. The bottom plot shows quite clearly that between maneuvers, the mean SMA often drifts above the target value. The mean SMA also occasionally drifts below the bottom of the control box. This occurs because the control logic requires the mean SMA at *apogee* to be less than $(6778 - \Delta a)$ km before a maneuver is performed. This requirement is not satisfied if the mean SMA drifts below the minimum value at other points in the orbit, but remains above it at apogee.

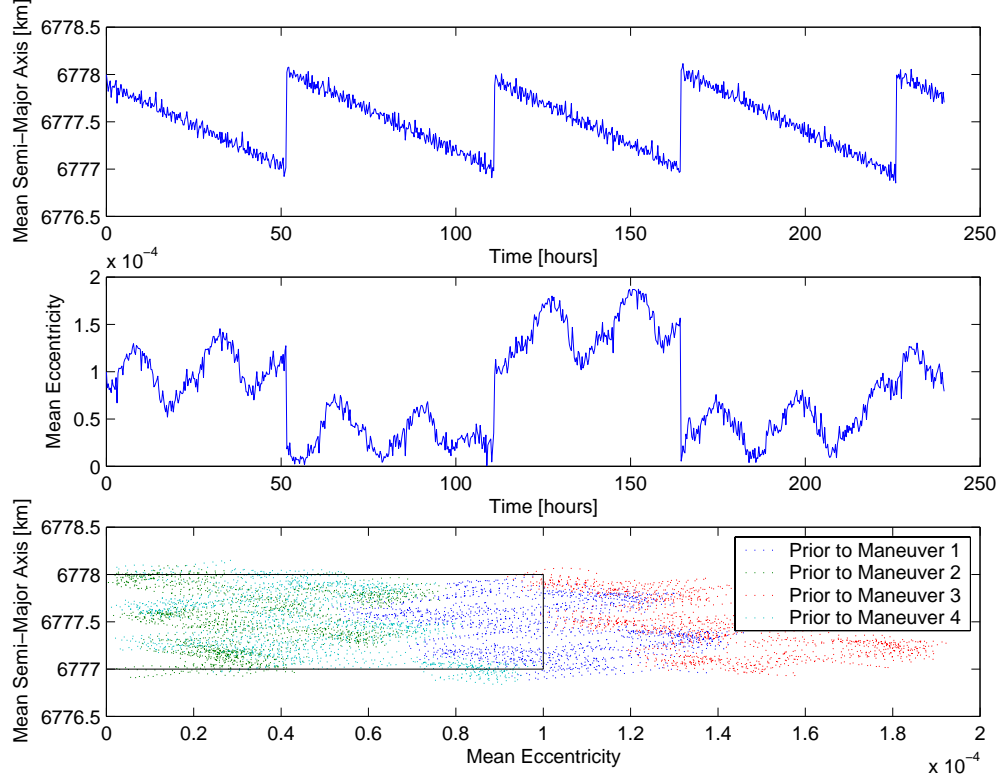


Figure 1: One-apogee-burn mean semi-major axis and mean eccentricity response with $\Delta a = 1$ km

Navigation

For the GPM onboard navigation analysis, we generate measurement data using the controlled trajectories described above. Changes to the Extended Kalman Filter used in previous cases include the addition of a *Maneuver* command, and an *Acceleration* command. These commands are sent to the filter whenever a maneuver occurs to allow the filter to increase the state covariance, and to include the thrust acceleration in the state propagation. For this analysis we do not include actuator noise at any stage, and thus the *Acceleration* command sent to the filter includes the exact applied control. Future work will include a realistic actuator noise model.

Table 4 shows navigation and control results for 10-day simulations of the 4 one-apogee-burn trajectories. Each trajectory includes 10 samples of Rubidium clock noise and pseudorange measurement noise. The values in the table are mean of mean, and mean of standard deviation values, as described above. Position and velocity mean errors for these scenarios increase with maneuver frequency. This is as expected as each maneuver results in a momentary increase in state covari-

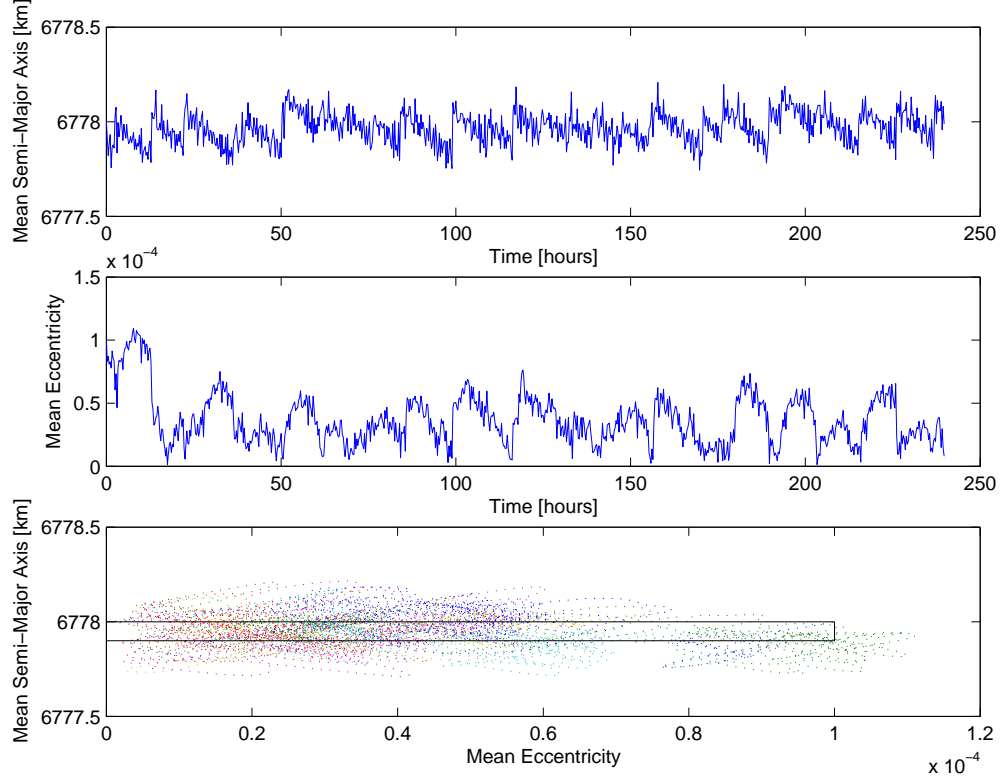


Figure 2: One-apogee-burn mean semi-major axis and mean eccentricity response with $\Delta a = 100$ m

ance, and increased state error. The position and velocity errors presented here are smaller than in real application as these simulations do not include GPS broadcast navigation ephemeris errors, or ionospheric delay.

Table 4: GPM one-apogee-burn mean results for 10-day, 10 sample run

Max Δa [m]	Number of Maneuvers	Total ΔV [m/s]	Position Error [m]		Velocity Error [cm/s]	
			mean	STD	mean	STD
1,000	4	2.295	1.955	0.707	0.277	0.089
500	8	2.399	1.973	0.717	0.297	0.095
100	29	2.439	2.072	0.851	0.319	0.121
10	84	2.413	2.320	1.119	0.412	0.185

The trend in the total ΔV results in Table 4 are somewhat surprising, as less frequent control appears to result in a decrease in total ΔV . We would expect that more frequent control would provide a significant fuel savings, as the spacecraft is not allowed to decay into the lower, more dense

atmosphere. This may be a result of the simulation time span being too short in comparison to the maneuver frequency of the large Δa cases. It is likely that a larger sampling of initial conditions, and longer simulation time spans would change this result less.

Conclusions

The two major goals of this project are: 1) to demonstrate the use of onboard navigation and control for a GPM drag compensation control strategy; 2) to determine the effect of drag-free control on GPS-based onboard navigation accuracy.

In order to demonstrate the use of onboard navigation and control for Global Precipitation Measurement (GPM), we have developed a simple guidance and control strategy which provides near-optimal* correction of the mean semi-major axis and mean eccentricity. Navigation results for a variety of scenarios show position error less than 5 m and velocity error less than 1 cm/s.

Drag-free trajectory analysis results show an improvement of less than 1% in estimated position accuracy when drag is removed. These results are primarily due to effective estimation of the drag coefficient error by GEONS. Further analysis is required to determine whether more realistic true drag (and thus greater drag model error) will result in more substantial navigation accuracy improvements.

*in the sense of the Hohmann transfer

Bibliography

- [1] Richard H. Battin. *An Introduction to the Mathematics and Methods of Astrodynamics, Revised Edition*. American Institute of Aeronautics and Astronautics, Inc, Reston, VA, 1999.
- [2] A. Long et al. Global Position System (GPS) Enhanced Onboard Navigation System (GEONS): Mathematical specifications. Computer Sciences Corporation Report CSC-5570-01R0UD0, Version 2, Release 2.0, Goddard Space Flight Center, Greenbelt, MD, February 2003.
- [3] David Folta and Albin Hawkins. Preliminary results of NASA's first autonomous formation flying experiment: Earth Observing-1 (EO-1). In *Flight Mechanics Symposium*, Goddard Space Flight Center, Greenbelt, MD, 2001.
- [4] Werner Gurtner. RINEX: The receiver independent exchange format version 2. Public ftp site, <ftp://ftp.geophys.washington.edu/pub/gps/RINEX-2.txt>, Astronomical Institute, University of Berne.
- [5] D. Kelbel. User's guide and mathematical specifications for the Measurement Data Simulation Program. Computer Sciences Corporation Report CSC-96-968-06, Goddard Space Flight Center, Greenbelt, MD, October 2000.
- [6] Jesse Leitner. Investigation of drag-free control technology for earth science constellation missions. Final Study Report, submitted to: NASA Earth Science Technology Office, May 15, 2003.
- [7] T. Mo and T. Lee. Analytic representation of the Harris-Priester atmospheric density model in the 110- to 2000-kilometers region. Prepared for Goddard Space Flight Center By Computer Sciences Corporation, Contract NAS 5-27600, October 1984.

- [8] Oliver Montenbruck and Eberhard Gill. *Satellite Orbits – Models, Methods, and Applications*. Springer Verlag, Heidelberg, Germany, 2000.